# Self-energy of a confined polaron in a quantum well: Comparison among different phonon models

Bao-Hua Wei* and Chang Sub Kim
*Department of Physics, Chonnam National University, Kwangju 500-757, Korea*
(Received 31 March 1998)

We study the interaction of an electron with the confined longitudinal optical phonons in quantum wells. For the Fröhlich interaction of the electron-phonons we adopt the Huang-Zhu [Phys. Rev. B **38**, 2183 (1988); **38**, 13 377 (1988)] confined phonon model based on a microscopic lattice-dynamic approach. The explicit expression for the electron self-energy is obtained using a variational method. We also use the slab model and the guided model for the confined optical phonons in calculating the electron self-energy. Consequently, a comparison of three models considered is provided. [S0163-1829(98)04535-4]

## I. INTRODUCTION

In recent years, there has been a great deal of interest in the study of the various vibrational modes in low-dimensional systems such as quantum wells, quantum wires, and superlattices.[1–9] The patterns of the normal modes that determine the electron-phonon interaction in such low-dimensional structures are evidently different from those in the bulk. The effect of quantum confinement alters the phonon modes and their interaction with electrons.

The widely used confined phonon modes in typical semiconductor quantum well structures such as GaAS/$Ga_{1-x}Al_xAs$ are the Fuchs-Kliewer *slab mode*[4] and the Ridley *guided mode*,[5] both of which are based on the macroscopic dielectric continuum model. However, use of these models for the description of the electron–LO-phonon (Fröhlich) interaction in quantum confined structures is still controversial.[6] Subsequently, several alternatives to the original Fuchs-Kliewer theory have been proposed.[10–16] Since there was no general consensus on which is the most suitable model, Rudin and Reinecke[10] and Weber and Ryan[11] had compared the three confined optical phonon modes in their study of the electron–LO-phonon scattering rate in the quantum wells. They found that the Huang-Zhu (HZ) model,[15,16] based on a microscopic lattice-dynamic description, is more appropriate than the slab model and guided model, in comparison to the existing experiments. Accordingly, it seems to be a worthwhile endeavor to compare further the various confined optical-phonon models for the different physical quantities.

In this work we report the results of our calculation of the electron self-energy for the electron-confined optical-phonon interaction in a quantum well structure. To the best of our knowledge, few people have used the HZ model to calculate the electron self-energy in quantum well structures. We also calculate the self-energy from the aforementioned two macroscopic models. Our results clearly manifest the differences among the three confined optical-phonon models.

The remainder of this paper is organized as follows. In Sec. II we write out the relevant Hamiltonians. In Sec. III we present the explicit expressions of the electron self-energy for three confined phonon models. Finally, the numerical results and associated discussion are given in Sec. IV.

## II. THREE CONFINED PHONON MODELS

We consider a quantum well model with width $a$, assuming that a polar crystal occupies the space for $|z| \leqslant a/2$ and the outside of the well is a vacuum. We restrict our interest to the influence of the electron-confined optical-phonon interaction to the electron self-energy. So the electron-electron and electron–interface-phonon interactions are neglected. Three different models for the confined optical phonons are treated. Within an isotropic effective mass ($m^*$) approximation, the Hamiltonian of the system can be deduced from Ref. 15 as

$$H=\frac{1}{2m^*}(\mathbf{p}_\parallel^2+p_z^2)+\sum_{q_\parallel,n}\hbar\omega_{LO}\beta^\dagger_{q_\parallel n}\beta_{q_\parallel n}+H_{e-ph}, \quad (1)$$

where

$$H_{e-ph}=\lambda\sum_{q_\parallel,n}e^{i\mathbf{q}_\parallel\cdot\mathbf{r}_\parallel}t_n(\mathbf{q}_\parallel)u_n(z)(\beta_{q_\parallel,n}+\beta^\dagger_{-q_\parallel,n}) \quad (2)$$

with

$$\lambda^2=\frac{4\pi\alpha}{V}(\hbar\omega_{LO})^2\sqrt{2\hbar/(m^*\omega_{LO})}.$$

In the above equations $\beta(\beta^\dagger)$ is the creation (annihilation) operator of the confined phonon with frequency $\omega_{LO}$, $n$ is the phonon-mode quantum number in the $z$ direction, $\mathbf{r}_\parallel$ and $\mathbf{p}_\parallel$ are the transverse coordinate and momentum, respectively, $\mathbf{q}_\parallel$ is the phonon wave vector in the $xy$ plane; $V$ is the volume of the crystal; and $\alpha$ is the electron-phonon coupling constant.

In the HZ microscopic model, the displacement $u_n(z)$ is given as

$$u_n(z)=\begin{cases}\sin(\mu_n\pi z)/a+(c_n z/a), & n=3,5,7,\ldots\\ \cos(n\pi z)/a+(-1)^{n/2+1}, & n=2,4,6,\ldots,\end{cases} \quad (3)$$

where $\mu_n$ are the solutions of the equation

$$\tan(\mu_n\pi/2)=(\mu_n\pi)/2, \quad n-1<\mu_n<n, \quad (4)$$

where

$$c_n=-2\ \sin(\mu_n\pi/2).$$

Here it is important to notice that the mode $n=1$ is excluded in the above equation because this mode is associated with the interface modes.[15]

In the slab model the electron potential has nodes at the interface and $u_n(z)$ takes the form[4]

 

$$u_n(z)=\begin{cases}\cos\dfrac{n\pi z}{a}, & n=1,3,5,\cdots\\ \sin\dfrac{n\pi z}{a}, & n=2,4,6,\ldots.\end{cases} \tag{5}$$

One can see that the $n$th mode of the slab model has an opposite parity to the that of the HZ model.

Based on the hydrodynamic boundary conditions proposed by Babiker[13] for longitudinal-optical phonons, the parity of the phonon modes of the guided model matches those obtained by the microscopic model. The displacement of the $n$th mode in the guided model is given as[5]

$$u_n(z)=\begin{cases}\sin\dfrac{n\pi z}{a}, & n=1,3,5,\ldots\\ \cos\dfrac{n\pi z}{a}, & n=2,4,6,\ldots.\end{cases} \tag{6}$$

Finally, $t_n(\mathbf{q}_\parallel)$ in Eq. (2) is defined as

$$t_n(\mathbf{q}_\parallel)=\left\{\frac{1}{a}\int_{-a/2}^{a/2}\left[q_\parallel^2u_n^2(z)+\left(\frac{du_n(z)}{dz}\right)^2\right]dz\right\}^{-1/2}. \tag{7}$$

An explicit calculation yields

$$t_n(\mathbf{q}_\parallel)=(a_nq_\parallel^2+b_n/a^2)^{-1/2}, \tag{8}$$

where $a_n$ and $b_n$ are for the Huang-Zhu model

$$a_n=1+c_n^2\left(\frac{1}{6}-\mu_n^{-2}\pi^{-2}\right),$$

$$b_n=\mu_n^2\pi^2-c_n^2,\quad n=3,5,7,\ldots \tag{9}$$

$$a_n=3,\quad b_n=n^2\pi^2,\quad n=2,4,6,\ldots$$

and for other two macroscopic models

$$a_n=1,\quad b_n=n^2\pi^2,\quad n=1,2,3,\ldots. \tag{10}$$

## III. SELF-ENERGIES OF THE ELECTRON

We use the Lee-Low-Pines method[17] to calculate the self-energy of the electron-confined optical-phonon interaction in the quantum well structures. To this end, we perform two unitary transformations with

$$U_1=\exp\left[-i\sum_{q_\parallel,n}\mathbf{q}_\parallel\cdot\mathbf{r}_\parallel\beta^\dagger_{k_\parallel,n}\beta_{k_\parallel,n}\right], \tag{11}$$

$$U_2=\exp\left[\sum_{q_\parallel,n}f_{q_\parallel,n}\beta^\dagger_{q_\parallel,n}-f^*_{q_\parallel,n}\beta_{q_\parallel,n}\right], \tag{12}$$

where $f_{q_\parallel,n}$ is the variational parameter, which will be subsequently determined by minimizing the energy of the system. The result of the first unitary transformation is

$$H'=U_1^{-1}HU_1=\frac{p_z^2}{2m^*}+\frac{1}{2m^*}\left(\mathbf{p}_\parallel-\sum_{k_\parallel n}\hbar\mathbf{q}_\parallel\beta^\dagger_{q_\parallel n}\beta_{q_\parallel n}\right)^2$$
$$+\sum_{q_\parallel,n}\hbar\omega_{LO}\beta^\dagger_{q_\parallel n}\beta_{q_\parallel n}+\lambda\sum_{q_\parallel,n}t_n(\mathbf{q}_\parallel)$$
$$\times u_n(z)[\beta_{q_\parallel n}+\beta^\dagger_{-q_\parallel n}]. \tag{13}$$

Using the relations for the second unitary transformation

$$U_2^+\beta_{q_\parallel n}U_2=\beta_{q_\parallel n}+f_{q_\parallel,n}, \tag{14}$$

$$U_2^+\beta^\dagger_{q_\parallel n}U_2=\beta^\dagger_{q_\parallel n}+f^*_{q_\parallel,n}, \tag{15}$$

we obtain

$$H''=U_2^{-1}H'U_2=H_0+H_1, \tag{16}$$

where

$$H_0=\frac{p_z^2}{2m^*}+\frac{1}{2m^*}\left(\mathbf{p}_\parallel-\sum_{k_\parallel,n}\hbar\mathbf{q}_\parallel\beta^\dagger_{q_\parallel n}\beta_{q_\parallel n}\right)^2+\sum_{q_\parallel,n}\hbar\omega_{LO}\beta^\dagger_{q_\parallel n}\beta_{q_\parallel n}+\sum_{q_\parallel,n}i\lambda[t_n(\mathbf{q}_\parallel)u_n(z)f_{q_\parallel,n}+t_n^*(\mathbf{q}_\parallel)u_n^*(z)f^*_{q_\parallel,n}]$$
$$+\frac{\hbar^2}{2m^*}\left[\sum_{q_\parallel,n}|f_{q_\parallel,n}|^2\mathbf{q}_\parallel\right]^2+\sum_{q_\parallel,n}|f_{q_\parallel,n}|^2\left[\hbar\omega_{LO}-\frac{\hbar\mathbf{q}_\parallel\cdot\mathbf{p}_\parallel}{m^*}+\frac{\hbar^2q_\parallel^2}{2m^*}\right]+\frac{\hbar^2}{m^*}\sum_{q_\parallel,n}\beta^\dagger_{q_\parallel n}\beta_{q_\parallel n}\mathbf{q}_\parallel\cdot\sum_{q'_\parallel,n'}[|f_{q'_\parallel,n'}|^2\mathbf{q}'_\parallel]$$
$$+\sum_{q_\parallel,n}\beta^\dagger_{q_\parallel n}\left\{i\lambda t_n^*(\mathbf{q}_\parallel)u_n^*(z)+f_{q_\parallel,n}\left[\hbar\omega_{LO}-\frac{\hbar\mathbf{q}_\parallel\cdot\mathbf{p}_\parallel}{m^*}+\frac{\hbar^2q_\parallel^2}{2m^*}+\frac{\hbar^2\mathbf{q}_\parallel}{m^*}\cdot\left(\sum_{q'_\parallel,n'}|f_{q'_\parallel,n'}|^2\mathbf{q}'_\parallel\right)\right]\right\}$$
$$+\sum_{q_\parallel,n}\beta_{q_\parallel n}\left\{-i\lambda t_n(\mathbf{q}_\parallel)u_n(z)+f^*_{q_\parallel,n}\left[\hbar\omega_{LO}-\frac{\hbar\mathbf{q}_\parallel\cdot\mathbf{p}_\parallel}{m^*}+\frac{\hbar^2q_\parallel^2}{2m^*}+\frac{\hbar^2\mathbf{q}_\parallel}{m^*}\cdot\left(\sum_{q'_\parallel,n'}|f_{q'_\parallel,n'}|^2\mathbf{q}'_\parallel\right)\right]\right\} \tag{17}$$

and

$$H_1=\sum_{q_\parallel,q'_\parallel,n,n'}\frac{\hbar^2\mathbf{q}_\parallel\cdot\mathbf{q}'_\parallel}{2m^*}[\beta^\dagger_{k_\parallel n}\beta_{q'_\parallel n'}f^*_{q_\parallel,n}f_{q'_\parallel,n'}+2\beta^\dagger_{q_\parallel n}\beta_{q'_\parallel n'}f_{q_\parallel,n}f^*_{q'_\parallel,n'}+\beta^\dagger_{q_\parallel n}\beta_{q'_\parallel n'}f_{q_\parallel,n}f_{q'_\parallel,n'}]$$
$$+\sum_{q_\parallel,q'_\parallel,n,n'}\frac{\hbar^2\mathbf{q}_\parallel\cdot\mathbf{q}'_\parallel}{m^*}[\beta^\dagger_{q_\parallel n}\beta_{q_\parallel n}\beta_{q'_\parallel n'}f^*_{q'_\parallel,n'}+\beta^\dagger_{q'_\parallel n'}\beta^\dagger_{q_\parallel n}\beta_{q_\parallel n}f^*_{q'_\parallel,n'}]. \tag{18}$$

Next, the expectation value of the transformed Hamiltonian is evaluated using the product wave function

$$|\psi\rangle = |\psi_m(z)\rangle|0\rangle, \tag{19}$$

where $|\psi_m(z)\rangle$ is the electron wave function with the subband index $m$ along the $z$ direction and $|0\rangle$ is the phonon vacuum state. In our infinite square well approximation, the electron wave functions are given as

$$|\psi_m(z)\rangle = \begin{cases} e^{i\mathbf{p}_\parallel\cdot\mathbf{r}_\parallel}\sqrt{2/V}\sin(m\pi z/a + m\pi/2), & |z| \leqslant a/2 \\ 0, & |z| > a/2 \end{cases} \tag{20}$$

where $m = 1,2,3,\ldots$ with the corresponding energies

$$E^0 = (\hbar^2 p_\parallel^2/2m^*) + (\hbar^2 m^2\pi^2/2m^* a^2). \tag{21}$$

The desired expectation value is

$$E = \langle\psi|H''|\psi\rangle = \langle\psi_m(z)|E(z)|\psi_m(z)\rangle, \tag{22}$$

where

$$E(z) = \frac{p_z^2}{2m^*} + \sum_{q_\parallel,n} i\lambda[t_n(\mathbf{q}_\parallel)u_n(z)f_{q_\parallel n} - t_n^*(\mathbf{q}_\parallel)u_n^*(z)f_{q_\parallel n}^*] + \frac{\hbar^2}{2m^*}\left[\sum_{q_\parallel,n}|f_{q_\parallel n}|^2\mathbf{q}_\parallel\right]^2 + \sum_{q_\parallel,n}|f_{q_\parallel n}|^2\left[\hbar\omega_{LO} + \frac{\hbar^2 q_\parallel^2}{2m^*}\right], \tag{23}$$

where we have dropped out terms associated with the electron momentum in the $xy$ plane because we are interested only in the ground state of the confined polaron. In the above equation, the term

$$\frac{\hbar^2}{2m^*}\left[\sum_{q_\parallel,n}|f_{q_\parallel n}|^2 q_\parallel\right]^2$$

describes the interaction between the virtual phonons emitted/absorbed by the recoiled electron, which is generally very small, especially in the weak coupling limit such as in the GaAs quantum well. Thus we will neglect this term in the following calculation.

Now we use the variational method to find out the unknown function $f_{q_\parallel n}$,

$$\frac{\delta E}{\delta f_{q_\parallel n}} = \frac{\delta E}{\delta f_{q_\parallel n}^*} = 0, \tag{24}$$

to get

$$f_{q_\parallel n}^* = \frac{-i\lambda t_n(\mathbf{q}_\parallel)\langle\psi_m(z)|u_n(z)|\psi_m(z)\rangle}{\hbar\omega_{LO} + \dfrac{\hbar^2 q_\parallel^2}{2m^*}}, \tag{25}$$

$$f_{q_\parallel n} = \frac{i\lambda t_n^*(\mathbf{q}_\parallel)\langle\psi_m(z)|u_n^*(z)|\psi_m(z)\rangle}{\hbar\omega_{LO} + \dfrac{\hbar^2 q_\parallel^2}{2m^*}}.$$

Substituting Eq. (25) into Eq. (22) and after a tedious but direct calculation, we finally obtain

$$E = \frac{\hbar^2 m^2\pi^2}{2m^* a^2} + E_{LO}, \tag{26}$$

where $E_{LO}$ is the electron self-energy, which is expressed as

$$E_{LO} = -\sum_{q_\parallel,n=3,5,7,\ldots,} \frac{\lambda^2 t_n^2(\mathbf{q}_\parallel)}{\hbar\omega_{LO} + \dfrac{\hbar^2 q_\parallel^2}{2m^*}}(I_1 + I_2 + I_3) - \sum_{q_\parallel,n=2,4,6,\ldots,} \frac{\lambda^2 t_n^2(\mathbf{q}_\parallel)}{\hbar\omega_{LO} + \dfrac{\hbar^2 q_\parallel^2}{2m^*}}[I_4 - 2(-1)^{n/2}I_5 + I_6]. \tag{27}$$

For the HZ model the functions $I_i$ are specified as

$$I_1 = \frac{1}{2} + \frac{m^2\sin(\mu_n\pi)}{2\pi\mu_n(\mu_n^2 - m^2)}, \tag{28}$$

$$I_2 = \frac{c_n^2}{12} - \frac{c_n^2}{2m^2\pi^2}, \tag{29}$$

$$I_3 = 8c_n m^2\left[\frac{\cos(\mu_n\pi/2)}{\pi(\mu_n^2 - 4m^2)} + \frac{(8m^2 - 6\mu_n^2)\sin(\mu_n\pi/2)}{\pi^2\mu_n(\mu_n^2 - 4m^2)^2}\right], \tag{30}$$

$$I_4 = \tfrac{1}{2} - \tfrac{1}{4}(-1)^n\delta_{nm}, \tag{31}$$

$$I_5 = \begin{cases} \dfrac{8m^2\sin(n\pi/2)}{n\pi(4m^2 - n^2)}, & n \neq 2m, \\ \dfrac{(-1)^{m+1}}{2}, & n = 2m, \end{cases} \tag{32}$$

$$I_6 = 1. \tag{33}$$

For the slab model they are given as

$$I_1 = \tfrac{1}{2} - \tfrac{1}{4}(-1)^n\delta_{nm}, \tag{34}$$

$$I_4 = \tfrac{1}{2} + \tfrac{1}{4}(-1)^n\delta_{nm}. \tag{35}$$

Similarly, for the guided model,

$$I_1 = \tfrac{1}{2} + \tfrac{1}{4}(-1)^n\delta_{nm}, \tag{36}$$

$$I_4 = \tfrac{1}{2} - \tfrac{1}{4}(-1)^n\delta_{nm}. \tag{37}$$

Notice that $I_2, I_3, I_5$ and $I_6$ are identically zero in both the slab and guided models.

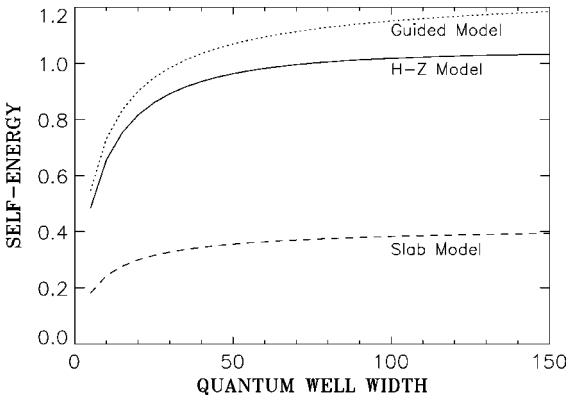


FIG. 1. Electron self-energies vs the quantum well width from three different confined phonon models; only the lowest subbands ($m=1$) are drawn. The self-energy and the well width are in units of $-\alpha\hbar\omega_{LO}$ and Å, respectively.

## IV. NUMERICAL RESULTS AND DISCUSSION

The numerical calculation is carried out using the material parameters suitable for the GaAs quantum well structures:[1] the electron-phonon coupling constant $\alpha=0.0657$; the effective conduction-band mass $m^*=0.0665m_0$, where $m_0$ is the bare mass of electron; and the LO-phonon energy $\hbar\omega_{LO}=36.7$ meV. We have calculated the electron self-energies for the three models considered for the confined optical phonons with varying well width.

In Fig. 1 we show the ground-state electron self-energies obtained as a function of the quantum well width for the different models of the confined optical phonons considered. The self-energy is normalized with respect to the limiting value of the bulk polaron, $-\alpha\hbar\omega_{LO}\doteq-2.41$ meV. The quantum confined behaviors are evident in the small well width region $a\leqslant 50$ Å for all three models. One can see that the absolute value of the self-energies of the HZ model is smaller than that of the guided model, but much larger than that of the slab model. This is attributed to the boundary conditions of the macroscopic models at the interface. In the slab model, the electrostatic boundary condition is used; consequently the phonon mode has the opposite parity to the microscopic mode. On the other hand, the guided model uses mechanical boundary condition, which makes its parity of the phonon modes match that of the microscopic model. Consequently, the difference between the HZ model and the slab model is bigger than that between the HZ model and the guided model. This renders one to imagine that a proper reformulation of the slab model may reduce the gap. In order to confirm this point, we have calculated the self-energy using the improved slab model by Weber,[18] modified to possess the same parity as the HZ model, to observe that the outcome is closer to the HZ model than even the guided model, not only its value but also the change with the quantum well width. The discrepancies between the HZ model and the guided model comes mainly from the fact that $n=1$ phonon mode, which belongs to the interface mode, is excluded in the former but the interface mode is included in the latter. Next, one may notice that three models tend to the different bulk limits at large well widths and only the HZ model tends to the proper bulk limit. This is because the slab model is restricted to the quasi-two-dimensional situation by construction[10]. The HZ model and the guided model can extend their validity to the large well width limit. However, because of the distinct mechanisms for the phonon modes used, there still exists the difference in the bulk values. We expect that an inclusion of the effect of the interface phonons will reduce the difference. We have seen the similar results for other subbands but not drawn.

## V. CONCLUSION

In conclusion, we have calculated the self-energies of the electron-confined LO-phonon interaction in the quantum well structure for three representative phonon models: the microscopic HZ model and the macroscopic slab and guided models. Our results show that the agreement between the HZ model and the guided model is better than that between the HZ model and the slab model. The discrepancy between the HZ model and guided model is attributed to the interface-phonon mode that is included in the guided model but not in the analytic approximation to the microscopic model. We have also confirmed that a proper reformulation of the slab model gives rise to the better agreement with the HZ model than the guided model.

## ACKNOWLEDGMENTS

This work was supported by the Ministry of Education of Korea through Grant No. BSRI-97-2431. B.-H.W. acknowledges support from GuangDong Provincial Natural Science Foundation of China.

*Permanent address: Department of Applied Physics, South China University of Technology, Guangzhou, China.

[1] J. T. Devreese and F. M. Peeters, *Polaron and Excitons in Polar Semiconductors and Ionic Crystals* (Plenum, New York, 1984).
[2] B. N. Onwuagba and B. H. Wei, Phys. Status Solidi B **190**, 151 (1995).
[3] M. A. Stroscio *et al.*, Superlattices Microstruct. **10**, 55 (1991).
[4] R. Fuchs and K. L. Kliewer, Phys. Rev. **140**, A2076 (1965).
[5] B. K. Ridley, Phys. Rev. B **39**, 5282 (1989).
[6] J. P. Leburton, J. Appl. Phys. **56**, 2850 (1984).
[7] R. Enderlein, Phys. Rev. B **47**, 2162 (1993).
[8] J. Shah *et al.*, Appl. Phys. Lett. **42**, 55 (1983).
[9] L. C. Chiu *et al.*, Jpn. J. Appl. Phys., Part 2 **22**, L82 (1983).
[10] S. R. Rudin and T. L. Reinecke, Phys. Rev. B **41**, 7713 (1990).
[11] G. Weber and J. F. Ryan, Phys. Rev. B **45**, 11 202 (1992).
[12] J. Menendez, J. Lumin. **44**, 285 (1989).
[13] M. Babiker, J. Phys. C **19**, 683 (1986).
[14] R. Chen *et al.*, Phys. Rev. B **41**, 1435 (1990).
[15] K. Huang and B. F. Zhu, Phys. Rev. B **38**, 2183 (1988); **38**, 13 377 (1988).
[16] B. F. Zhu, Phys. Rev. B **38**, 7694 (1988); **44**, 1926 (1991).
[17] T. D. Lee *et al.*, Phys. Rev. **90**, 297 (1953).
[18] G. Weber, Phys. Rev. B **46**, 16 171 (1992).